

PicT: A Slim Weakly Supervised Vision Transformer for Pavement Distress Classification

Wenhao Tang

School of Big Data & Software Engineering, Chongqing University
Chongqing, China
whtang@cqu.edu.cn

Xiaoxian Zhang

School of Big Data & Software Engineering, Chongqing University
Chongqing, China
zhangxiaoxian@cqu.edu.cn

Sheng Huang*

School of Big Data & Software Engineering and Ministry of Education Key Laboratory of Dependable Service Computing in Cyber Physical Society, Chongqing University
Chongqing, China
huangsheng@cqu.edu.cn

Luwen Huangfu

Fowler College of Business and Center for Human Dynamics in the Mobile Age, San Diego State University
San Diego, California, USA
lhuangfu@sdsu.edu

ABSTRACT

Automatic pavement distress classification facilitates improving the efficiency of pavement maintenance and reducing the cost of labor and resources. A recently influential branch of this task divides the pavement image into patches and infers the patch labels for addressing these issues from the perspective of multi-instance learning. However, these methods neglect the correlation between patches and suffer from a low efficiency in the model optimization and inference. As a representative approach of vision Transformer, Swin Transformer is able to address both of these issues. It first provides a succinct and efficient framework for encoding the divided patches as visual tokens, then employs self-attention to model their relations. Built upon Swin Transformer, we present a novel vision Transformer named **Pavement Image Classification Transformer (PicT)** for pavement distress classification. In order to better exploit the discriminative information of pavement images at the patch level, the *Patch Labeling Teacher* is proposed to leverage a teacher model to dynamically generate pseudo labels of patches from image labels during each iteration, and guides the model to learn the discriminative features of patches via patch label inference in a weakly supervised manner. The broad classification head of Swin Transformer may dilute the discriminative features of distressed patches in the feature aggregation step due to the small distressed area ratio of the pavement image. To overcome this drawback, we present a *Patch Refiner* to cluster patches into different groups and only select the highest distress-risk group to yield a slim head for the final image classification. We evaluate our method on a large-scale bituminous pavement distress dataset named CQU-BPDD. Extensive results demonstrate the superiority of our method over baselines and also show that **PicT** outperforms the second-best performed model by a large margin of +2.4% in P@R on detection task, +3.9% in F1 on recognition task, and 1.8x throughput, while enjoying 7x faster training speed using the same computing resources. Our codes and models have been released on <https://github.com/DearCaat/PicT>.

*indicates the corresponding author.

CCS CONCEPTS

• **Computing methodologies** → **Object identification**; *Computer vision tasks*; **Object recognition**.

KEYWORDS

Pavement Distress Classification, Deep Learning, Image Classification, Transformers, Weakly Supervised Learning

1 INTRODUCTION

With the rapid growth of transport infrastructures such as airports, bridges, and roads, pavement maintenance is deemed as a crucial element of sustainable pavement today [42]. It is a trend to automate this process via machine learning and pattern recognition techniques, which can significantly reduce the cost of labor and resources. One of the core tasks in pavement maintenance is pavement distress classification (PDC), which aims to detect the damaged pavement and recognize its specific distress category. These two steps are also referred to as pavement distress detection and pavement distress recognition, respectively [20].

For decades, many researchers have been devoted to investigate PDC from the perspective of computer vision. The traditional methods are to utilize image processing, hand-craft features, and conventional classifiers to recognize the pavement distress [3, 25, 36, 45]. The main drawback of these methods is that they highly rely on expert knowledge and suffer from the weak generalization ability [6]. Inspired by the recent remarkable successes of deep learning, many deep learning-based approaches have been proposed for addressing the PDC issue [8, 12, 22]. However, these methods often regard the PDC problem as a common image classification problem, while seldom paying attention to the specific characteristics of pavement images, such as the high image resolution, the low distressed area ratio, and uneven illumination, in the model design phase [19].

To consider these characteristics of pavement images, some of the latest approaches [19, 20, 33] attempt to divide the high-resolution raw pavement image into patches and solve this problem via inferring the labels of patches with CNNs as shown in Figure 2. Intuitively, these approaches can be deemed as a kind of multi-instance

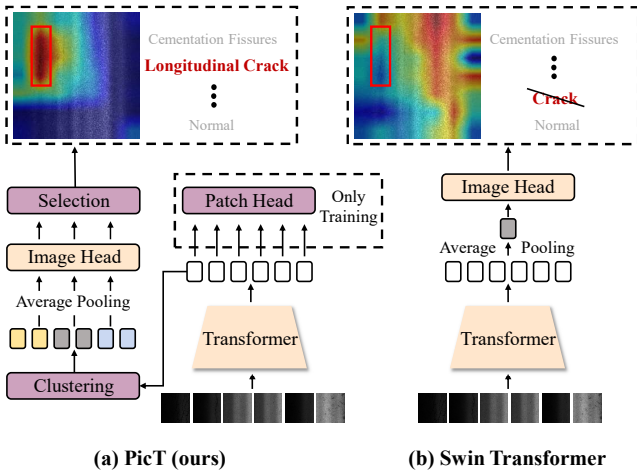


Figure 1: (a) The proposed PicT aims to learn the discriminative information of patches via performing the patch classification in a weakly supervised manner while employing a slim image classification head to select the features of the highest risk patches only for achieving a better distress classification. (b) In contrast, the general vision Transformer, like Swin Transformer, fails to mine the local discriminative features, and locate the distressed area. Moreover, its classifier is easy to be fooled by the overabundant features of non-distressed patches due to the small distressed area ratio property of pavement images.

learning approach [5], merited by their ability to better learn the local discriminative information of the high-resolution image and thereby achieve promising performances. For example, IOPLIN [33] conducts the feature extraction and classification on each patch independently and finally aggregates the classification results via max-pooling or average-pooling. Similarly, WSPLIN [19, 20] also extracts the feature of each patch and classifies the patch independently. However, instead of conducting the classification result aggregation, it inputs the classification results of all patches into a comprehensive decision network for accomplishing the final classification. Generally speaking, the whole patch label inference process, including patch partition, feature extraction, and classification is quite expatiatory, which leads to the low efficiencies of these approaches. What’s more, the patches naturally have correlation while these methods all neglect this nature.

Recently, the vision Transformer has demonstrated excellent performances in supervised learning [11, 27, 37, 41], weakly supervised learning [10, 28], and self-supervised learning tasks [16, 38]. Its success is benefited from the self-attention mechanism [35] and the strong local representation capability. As an influential approach in vision Transformer, Swin Transformer [24] shares a similar idea as the aforementioned patch-based PDC in the visual information exploitation. It also partitions the image into different patches and encodes them as visual tokens. Then, self-attention is employed to model their relations. Finally, these tokens are aggregated for yielding the final classification. Compared to previous approaches, the vision Transformer provides a more succinct and advanced framework for learning the subtle discriminative features of images as shown in Figure 2 (a). However, it is still inappropriate to

directly apply Swin Transformer to address the PDC issue for two reasons. The first one is that the potential discriminating features of patches are still not well explored as the CAMs shown in Figure 1 (b), since the patch-level supervised information has still not been sufficiently mined in the Swin Transformer. The second reason is that its average-pooling aggregation for all patches will suppress the distressed patch features, since the distressed patches are only a small fraction of all patches.

In this paper, we elaborate on a novel Transformer named **PicT** which stands for **Pavement Image Classification Transformer**, based on the Swin Transformer framework for Pavement Distress Classification (PDC). In order to overcome the first drawback of the Swin Transformer in PDC, we develop a *Patch Labeling Teacher* module based on the idea of teacher-student model to present a weakly supervised patch label inference scheme for fully mining the discriminative features of patches. In order to overcome the second drawback of the Swin Transformer in PDC, a *Patch Refiner* module is designed to cluster the patches and select the patches from the highest risk cluster to yield a slimmer head for final classification. This strategy can significantly suppress the interferences from the plentiful non-distressed (normal) patches in the image label inference phase. A large-scale pavement image dataset named CQU-BPDD is adopted for evaluation. Extensive experiments demonstrate that PicT achieves state-of-the-art performances in two common PDC tasks, namely pavement distress detection, and pavement distress recognition. More importantly, PicT outperforms the second-best performed model by a large margin of +2.4% in P@R on detection task, +3.9% in F1 on recognition task, and 1.8x throughput, while enjoying 7x faster training efficiency.

The main contributions of our work are summarized as follows:

- We propose a novel vision Transformer named PicT for pavement distress classification. PicT not only inherits the merits of Swin Transformer but also takes the characteristics of pavement images into consideration. To the best of our knowledge, it is the first attempt to specifically design a Transformer to address pavement image analysis issues.
- A *Patch Labeling Teacher* module is elaborated to learn to infer the labels of patches in a weakly supervised fashion. It enables better exploiting the discriminative information of patches under the guidance of the patch-level supervised information, which is generated by a *Prior-based Patch Pseudo Label Generator* based on image labels. Such an idea can also be flexibly applied to other vision Transformers to infer labels of visual tokens in a weakly supervised manner.
- A *Patch Refiner* is designed to yield a slimmer head for PDC. It enables filtering out the features from low-risk patches while preserving the ones from high-risk patches to boost the discriminating power of the model further.
- We systematically evaluate the performances of common vision Transformers on two pavement distress classification tasks. Extensive results demonstrate the superiority of PicT over them. Compared to the second-best performed method, PicT achieves 2.4% more detection performance gains in P@R, 3.9% recognition performance gains in F1, 1.8x higher throughput, and 7x faster training speed.

2 RELATED WORK

2.1 Pavement Distress Classification

Pavement Distressed Classification (PDC) aims to detect the diseased pavement and recognize the specific distress category of pavements with pavement images. The traditional methods are to utilize image processing, hand-craft features, and conventional classifiers to recognize the pavement distress [3, 25, 36, 45]. The main drawback of these methods is that they rely on expert knowledge and suffer from the weak generalization ability [6].

Inspired by the recent remarkable successes of deep learning in extensive applications, simple and efficient convolutional neural networks (CNN) based PDC methods have gradually become the mainstream in recent years. There are two major branches: one is the general-CNN methods and the other is patch-based methods. The general-CNN approaches [8, 12, 22] only regard the PDC as a standard image classification problem and directly apply the classical deep learning approaches to solve it. For example, [22] proposes a novel method using deep CNN to automatically classify image patches cropped from 3D pavement images and successfully trains four supervised CNNs with different sizes of receptive field. However, general-CNN methods seldom paid attention to the specific characteristics of pavement images. Patch-based methods [19, 20, 33] have addressed these issues by splitting the patches and inferring the labels of patches. IOPLIN [33] manually partitions the high-resolution pavement image into patches and elaborates an iteratively optimized CNN model to predict patch labels for detection. It enables learning the discriminative details of the local regions and then improves the performance. WSPLIN [19, 20] conducts the same process as IOPLIN but uses a comprehensive decision network to aggregate the classification results of patches for accomplishing the final image classification. However, the whole image partition, patch feature extraction, and classification process often necessitates a large burden in efficiency. Moreover, such methods often neglect the correlation between patches.

2.2 Vision Transformer

Transformer origins from natural language processing and machine translation [4, 35]. Recently, they have been successfully applied to many computer vision domains [2, 14, 23, 40, 41, 43]. Generally speaking, the Transformer models in the computer vision community can be roughly divided into two groups: combining self-attention with CNN [9, 11, 27, 37] and vision Transformer models [7, 24, 38, 39]. The first type of method focuses on using powerful self-attention mechanism to model the correlation between features extracted by CNN. For example, Girdhar et al. [11] repurpose a Transformer-style architecture to model features from the spatiotemporal context around the person whose actions are attempted for classification. On the other hand, with the release of ViT [7], more and more work apply vision Transformer to achieve better results in different vision areas [1, 10, 15, 16, 18, 24, 38, 39]. For example, LOST [28] achieves SOTA on objective search by combining similar tokens and using seed search to complete the object localization. SimMM [38] predicts raw pixel values of the randomly masked patches by a lightweight one-layer head and performs learning using a simple L1 loss. In particular, these outstanding studies in the field of weakly supervised localization [10, 28] and

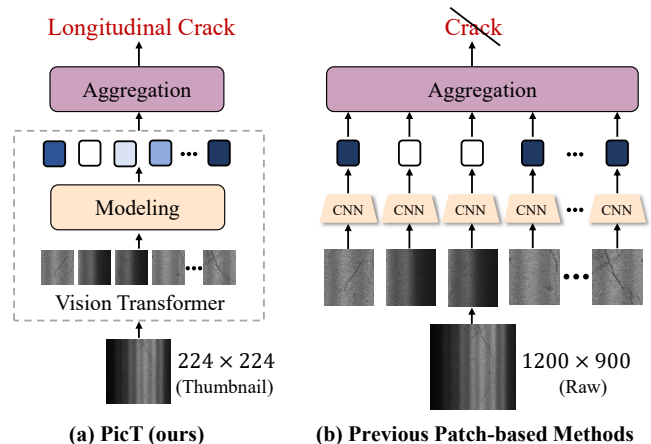


Figure 2: (a) The PicT is a more succinct and efficient learning framework based on the vision Transformer and leverages the self-attention module to model the correlation between patches. (b) In contrast, because CNN lacks the ideal inter-local correlation modeling capability and struggles to capture the subtle discriminative features, previous patch-based methods have to manually split the high-resolution raw image into patches. This leads to lower efficiency and the neglect of the patch correlation.

self-supervised learning [1, 16, 38] demonstrate the powerful local representation capabilities of tokens in vision Transformer models. In this work, we attempt to leverage the merits of Transformer for addressing the PDC issue.

3 METHOD

3.1 Problem Formulation and Overview

3.1.1 Problem Formulation. Pavement Distress Classification (PDC) can be deemed as an image classification task from the perspective of computer vision. Let $X = \{x_1, \dots, x_n\}$ and $Y = \{y_1, \dots, y_n\}$ be the collection of pavement images and their pavement labels respectively, where y_i is a C -dimensional vector and C is the number of categories. Let the subset $Y_{nor} \in Y$ be the non-distressed label set and $Y_{dis} \in Y$ be the distressed label set, which indicate the presence or absence of distress in a pavement image. Pavement distress detection and recognition are the most common tasks in the PDC. The pavement distress detection task is a binary image classification issue ($C = 2$), which judges if a pavement image exists distress or not, while the pavement distress recognition task is a multi-class image classification problem ($C > 2$) which classifies the pavement image into a specific distress category. In this paper, we develop a novel vision Transformer model named PicT for addressing the aforementioned PDC issues both.

3.1.2 Overview. The overview of PicT is shown in Figure 3. This entire framework is based on the well-known Swin Transformer. In order to incorporate the specific characteristics of pavement images, such as the high resolution and the low distressed area ratio, we enhance Swin Transformer by introducing two elaborate modifications. We borrow the idea from self-supervised learning to develop a *Patch Labeling Teacher* (PLT) for better exploring the discriminating power of patch information via classifying patches

3.3 Prior-based Patch Pseudo Label Generator

The performance of the patch classifier highly relies on the quality of the generated pseudo-label [39]. So, we propose a *Prior-based Patch Pseudo Label Generator* (P³LG) to accomplish this task with the help of the prior information, such as image labels, distressed area ratio, and the patch label predictions dynamically produced by the teacher model. P³LG consists of two important steps: Relative Distress Threshold and Patch Filter.

3.3.1 Relative Distress Threshold (RDT). A Relative Distress Threshold (RDT) is defined for producing the pseudo labels of patches. In RDT, the patch pseudo labels are always fixed to the normal one, y_{normal} , if the pavement image has no distress ($y_i \in Y_{nor}$). While the patches, which own the top $\Delta_{rel}\%$ highest predictions of the image distress label y_i , will be considered as the patches owning the distressed category y_i , if the distressed label of the pavement image is y_i . The whole strategy can be mathematically denoted as follows,

$$\hat{y}_{ij} = \begin{cases} y_i, & p_{ij}^{y_i} > \mathcal{T}(\Delta_{rel}) \text{ and } y_i \in Y_{dis} \\ y_{normal}, & \text{others,} \end{cases} \quad (4)$$

where $p_{ij}^{y_i}$ is the element of patch label predictions corresponding to the distressed category of y_i , and $\mathcal{T}(\Delta_{rel})$ returns the $\Delta_{rel}\%$ largest $p_{ij}^{y_i}$ of all patches in image x_i . Compared with the common absolute threshold strategy [21], this threshold enables ensuring that a distressed image always has a certain percentage of distressed instances. This also alleviates the pseudo-label bias caused by inconsistent training of the model for different distress categories.

3.3.2 Patch Filter. Following [39], we filter out low prediction confidence patches, and only preserve the high confidence ones for training.

- For **Distressed Image**: We preserve all patches whose pseudo-labels are not y_{normal} , and also preserve the patches whose pseudo-labels are y_{normal} and $p_{ij}^{y_{normal}} > 0.5$.
- For **Non-distressed Image**: We only preserve the high prediction confident patches whose $p_{ij}^{y_{normal}} > 0.95$.

These two optimal patch filtering thresholds are obtained in an empirical way.

3.4 Patch Refiner

After the feature extraction of patches, these features will be aggregated via average-pooling overall patches, and then performed for classification in the Swin Transformer. However, the distressed patches are only a small fraction of overall patches, so this feature aggregation strategy is easy to dilute the discriminative features of distressed patches. In order to address this issue, we develop a *Patch Refiner* (PR) to yield a slimmer image head.

Let $\mathcal{R}_\xi(\cdot)$ be the mapping function of PR where ξ is its parameters. It consists of three steps, namely token clustering, aggregation, and selection. The mapping functions of these steps are denoted as $f_{clu}(\cdot)$, $h^{img}(\cdot)$, and $f_{sel}(\cdot)$ respectively. So $\mathcal{R} = f_{sel} \circ h^{img} \circ f_{clu}$. Compared with the image head in Swin Transformer, which aggregates all tokens for classification, our image head is a much slimmer head, since it only highlights the highest risk group of tokens for conducting the final classification.

In *Patch Refiner*, the tokens are first clustered into different groups via using K-Means [13]. Then the average-pooling is conducted on each group for feature aggregation, and these aggregated features will be input into an image head for assessing the distressed risk of each group. The whole process can be mathematically represented as follows,

$$R_i = h^{img}(f_{clu}(T_i)) = \{r_{i1}, \dots, r_{it}, \dots, r_{ik} \mid r_{it} \in \mathbb{R}^C\}, \quad (5)$$

where R_i is the label predictions of groups, and k is the group number. r_{it} is the label predictions of the t -th group, which can be deemed as the risk assessments of different distresses for this group. In our approach, k is empirically fixed to 2 for the detection task while 3 for the recognition task.

In the image label classification phase, we intend to suppress the interferences from the overabundant non-distressed patches. So, we only select the highest risk group to represent the pavement image for final classification. In other words, we only preserve the label predictions of the group, which owns the lowest confident label prediction in the normal (non-distressed) category, as the predicted labels of image \hat{y}_i ,

$$\hat{y}_i = \mathcal{R}(T_i) = f_{sel}(R_i) = \arg \min_{r_{it}} \{r_{it}^{y_{normal}} \mid r_{it} \in R_i\}, \quad (6)$$

where $r_{it}^{y_{normal}}$ is the element of r_{it} corresponding to the normal category. Once we obtain the predicted labels of images, we can use the cross-entropy to measure the image classification loss,

$$\mathcal{L}_i = -\frac{1}{n} \sum_{i=1}^n y_i \log \hat{y}_i. \quad (7)$$

Finally, the optimal PicT model can be learned by minimizing both the patch and image classification losses,

$$(\hat{\theta}_s, \hat{\xi}) \leftarrow \arg \min_{\theta_s, \xi} \mathcal{L}_{total} := \mathcal{L}_i + \mathcal{L}_p. \quad (8)$$

3.5 Pavement Distress Classification

To tackle pavement distress classification, we can train our model as a pavement image classifier. Once the model is trained, the pavement image x_i can be fed into PicT for yielding the final classification result. Of particular interest, although we use patch-level branch named *Patch Labeling Teacher* to enhance the use of patch information in the training process. But in the testing phase, we only leverage the image-level branch named *Patch Refiner* for model inference due to the instability of patch-level testing. The process of PDC can be denoted as:

$$y_i = \mathcal{R}(f(x_i)) = f_{sel}(h^{img}(f_{clu}(f(x_i))))). \quad (9)$$

Note, the selection $f_{sel}(\cdot)$ in the testing phase is slightly different from it in training phase. More details about this will be specified in the support material.

4 EXPERIMENTS

4.1 Dataset and Setup

4.1.1 Task Settings. Following [20], we evaluate our method on pavement distress detection and recognition tasks under two application settings. The first one is the one-stage detection (**I-DET**), which is the conventional detection fashion. In this setting, the model only needs to determine whether there are distressed areas

Table 1: The pavement distress detection performances of different approaches on the CQU-BPDD. P@R = $n\%$ indicates the precision when the corresponding recall is equal to $n\%$. The best performances are in bold, and the second-best results are underlined.

| Detectors(I-DET) | AUC | P@R=90% | P@R=95% |
|----------------------|--------------|--------------|--------------|
| ResNet-50 [17] | 90.5% | 45.0% | 35.3% |
| Inception-v3 [31] | 93.3% | 56.0% | 42.3% |
| VGG-19 [29] | 94.2% | 60.0% | 45.0% |
| EfficientNet-B3 [32] | 95.4% | 68.9% | 51.1% |
| ViT-S/16 [7] | 95.4% | 67.7% | 51.0% |
| ViT-B/16 [7] | 96.1% | 71.2% | 56.1% |
| DeiT-S [34] | 95.5% | 68.2% | 52.2% |
| DeiT-B [34] | 96.3% | 75.2% | 59.3% |
| Swin-S [24] | 97.1% | 79.9% | 65.5% |
| IOPLIN [33] | 97.4% | 81.7% | 67.0% |
| WSPLIN-IP [20] | <u>97.5%</u> | <u>83.2%</u> | <u>69.5%</u> |
| PicT (ours) | 97.9% | 85.6% | 75.2% |

| Recognizers(I-REC) | AUC | P@R=90% | P@R=95% |
|----------------------|--------------|--------------|--------------|
| EfficientNet-B3 [32] | 96.0% | 77.3% | 59.9% |
| Swin-S [24] | 97.2% | 82.7% | 69.0% |
| WSPLIN-IP [20] | <u>97.6%</u> | <u>85.3%</u> | <u>72.6%</u> |
| PicT (ours) | 98.1% | 87.6% | 77.0% |

in the pavement image. The second one is the one-stage recognition (**I-REC**), which tackles the pavement distress detection and recognition tasks jointly. In this setting, the model not only detects the presence of distressed areas within the pavement image, but also needs to further classify the distressed category. Compared to **I-DET**, this task is more challenging and practically applicable. Moreover, both the detection and recognition performances can be evaluated in this setting.

4.1.2 Datasets. Before [33], most of the methods in the PDC are validated on private datasets. Thus, following [33], a large-scale public bituminous pavement distress dataset named CQU-BPDD [33] is used for evaluation. This dataset involves seven different types of distress and non-distressed categories. There are 10137 images in the training set and 49919 images in the test set only with the image-level labels. For the setting of **I-DET**, only the binary coarse-grained category label (distressed or normal) is available. For the setting of **I-REC**, their fine-grained category labels are available for training and testing models.

4.1.3 Evaluation Protocols and Metrics. Following the standard evaluation protocol in [33], for **I-DET** task, we adopt Area Under Curve (AUC) of Receiver Operating Characteristic (ROC) and Precision@Recall (P@R) to evaluate the model performance. The AUC is the common metric in binary classification task. P@R is used to discuss the precision under high recall, which is more meaningful in the medical or pavement distress classification tasks. Since the miss of the positive samples (the distressed sample) may lead to a more severe impact than the miss of the negative ones. As for **I-REC** task, following [20], we use the Top-1 accuracy and Marco F1 score ($F1$) to evaluate the performance of the models. Please refer to Supplementary for the details of implementation.

Table 2: The pavement distress recognition performances of different methods. $F1$ indicates the Marco $F1$ -score.

| Recognizers(I-REC) | Top-1 | $F1$ |
|----------------------|--------------|--------------|
| ResNet-50 [17] | 88.3% | 60.2% |
| VGG-16 [29] | 87.7% | 58.4% |
| Inception-v3 [31] | 89.3% | 62.9% |
| EfficientNet-B3 [32] | 88.1% | 63.2% |
| ViT-S/16 [7] | 86.8% | 59.0% |
| ViT-B/16 [7] | 88.1% | 61.2% |
| DeiT-S [34] | 88.3% | 60.7% |
| DeiT-B [34] | 89.1% | 62.7% |
| Swin-S [24] | 89.5% | 64.9% |
| WSPLIN-IP [20] | <u>91.1%</u> | <u>66.3%</u> |
| PicT (ours) | 92.2% | 70.2% |

4.2 Pavement Distress Detection

Table 1 tabulates the pavement distress detection performances of different methods on **I-DET** and **I-REC** settings. The observations demonstrate that PicT outperforms all the compared methods on both **I-DET** and **I-REC** settings under all evaluation metrics. Swin-S is adopted as the backbone of PicT. The performance gains of PicT over it are 0.8%, 5.7%, and 9.7% in AUC, P@R=90%, and P@R=95% respectively in the **I-DET** setting. These numbers on **I-REC** settings are 0.9%, 4.9%, and 8.0% respectively. These results validate the effectiveness of our modification in Swin-S according to the characteristics of the pavement images. Moreover, even though Swin-S adopts a more powerful learning framework (Transformer) and also can be deemed as a patch-based approach, it still cannot defeat the conventional patch-based methods, such as WSPLIN and IOPLIN. This phenomenon reflects that it is inappropriate to directly apply Swin-S for PDC, and further confirms that it is important to incorporate the characteristics of pavement images in the model design phase.

WSPLIN is the second-best approach for pavement distress detection. Our method still gets considerable advantages in performance over it. For example, the performance gains of PicT over WSPLIN are 0.4%, 2.4%, and 5.7% in AUC, P@R=90%, and P@R=95% respectively on **I-DET** setting. In the **I-REC** setting, these numbers are 0.5%, 2.3%, and 4.4% respectively. These results verify the advantages of the Swin Transformer framework over the conventional CNN-based learning framework in pavement distress detection.

4.3 Pavement Distress Recognition

Table 2 reports the pavement distress recognition performances on the CQU-BPDD dataset. We can observe similar phenomena as the ones observed in pavement distress detection. PicT still outperforms all approaches in pavement distress recognition, which is considered a more challenging PDC task than pavement distress detection. The results show that our method even holds the more prominent advantages in performance compared with the ones of pavement distress detection. For example, the performance gains of PicT over Swin-S are 2.7% and 5.3% in Top-1 and $F1$, respectively, while the number of PicT over WSPLIN are 1.1% and 3.9% respectively. Clearly, all observations well verify the arguments we raised in Section 4.2.

Table 3: The training and inference efficiencies of different patch-based approaches. TrainTime is the total training time on one RTX3090 GPU. Throughput is measured on RTX3090 GPU FP32 with batch size 1.

| Method | I-DET (P@R=90%) | I-REC (F1) | TrainTime (h) | Throughput (imgs/sec) |
|----------------|--------------------|---------------|------------------|--------------------------|
| Effi-B3 [32] | 68.9% | 63.2% | (+00%) 0.7h | (1.0x) 75 |
| Swin-S [24] | 79.9% | 64.9% | (+14%) 0.8h | (0.8x) 62 |
| WSPLIN-IP [20] | 83.2% | 66.3% | (+00%) 11.1h | (1.0x) 31 |
| IOPLIN [33] | 81.7% | - | (+13%) 12.5h | (1.4x) 43 |
| WSPLIN-SS [20] | 81.4% | 64.1% | (-49%) 5.7h | (1.7x) 53 |
| PicT (ours) | 85.6% | 70.2% | (-87%) 1.5h | (1.8x) 57 |

Table 4: The ablation study results of the proposed model. The backbone is Swin-S, and PicT=Patch Labeling Teacher + Patch Refiner.

| Method | I-DET (P@R=90%) | I-REC (F1) |
|--|--------------------|---------------|
| Swin-S [24] | 79.9% | 64.9% |
| Patch Refiner | 84.1% | 67.0% |
| Patch Labeling Teacher | 81.7% | 67.3% |
| Patch Labeling Teacher + Swin-S | 85.1% | 67.9% |
| Patch Labeling Teacher + Patch Refiner | 85.6% | 70.2% |

4.4 Efficiency Evaluation

We tabulate the training and inference efficiencies of the patch-based approaches and also their backbone networks along with their classification performances in Table 3. Patch-based approaches include our proposed PicT, WSPLIN, and IOPLIN. We report the efficiencies of two WSPLIN approaches, namely WSPLIN-IP (the default version) and WSPLIN-SS (the speed-up version). The backbone of PicT is Swin-S while the backbones of other patch-based approaches are EfficientNet-B3 (Effi-B3). From observations, we can see that Effi-B3 slightly performs better than Swin-S in efficiency. Swin-S needs 14% more time for training the model with the same computing resources. Even so, PicT still shows significant advantages over other patch-based approaches in efficiency. For example, the training speed of PicT is around 7x, 8x, and 4x faster than the ones of WSPLIN-IP, IOPLIN, and WSPLIN-SS respectively. PicT can accomplish the label inferences of 26 more images, 14 more images, and 4 more images per second over WSPLIN-IP, IOPLIN, and WSPLIN-SS respectively. We attribute the good efficiency of PicT to the succinct learning framework of Swin-S. Besides the superiority in efficiency, PicT also holds a significant advantage in performance. For instance, WSPLIN-SS is the fastest patch-based approach except for PicT. PicT obtains 4.2% and 6.1% more performances than WSPLIN-SS in P@R=90% and F1 respectively. To sum up, PicT is superior to the other patch-based approaches no matter in both performance and efficiency.

4.5 Ablation Study

4.5.1 Impacts of Different Modules. Table 4 reports the performances of PicT under different settings in modules. Swin-S is the backbone of PicT, which is considered the baseline. *Patch Refiner* and *Patch Labeling Teacher* respectively indicate the PicT models only use our proposed image-level classification branch and our

proposed patch-level classification branch. *Patch Labeling Teacher* + Swin-S indicates the models use two classification branches. One is our proposed patch-level classification branch, and the other is the original image head of Swin-S (the broad head). *Patch Labeling Teacher* + *Patch Refiner* is the final PicT model, which has two classification branches. One is our proposed patch-level classification branch, and the other is our proposed image-level classification branch (the slim head). From observations, we can find that all two proposed modules improve the performances of the baseline no matter if used independently or in a combined way. These results verify our argument that further exploiting the discriminative information of patches via the patch-level supervision and highlighting the discriminative features of distressed patches can assist Swin-S in better addressing the PDC issue.

4.5.2 Discussion on Hyperparameters. There are two tunable hyperparameters in our model. One is the cluster number k in *Patch Refiner*, which determines how many patches will be filtered out. The other is Δ_{rel} in the Relative Distress Threshold (RDT) of *Patch Labeling Teacher*, which determines how many high-risk patches should be preserved in a distressed pavement image. Figures 5 and 6 respectively plot the relationships between the performances of PicT and the values of these hyperparameters. We can observe that the PicT performs much better with a relatively smaller k . We attribute this to the fact that a larger k is easy to cause the overmuch information loss in image-level classification, since only about $\frac{1}{k}$ of the patches have been preserved for taking part in the final classification. Similar phenomenon can be also observed on Δ_{rel} . The reason why the relatively smaller Δ_{rel} often achieves a better performance is that the distressed area of pavement image is often very small and most of the patches are actually non-distressed, even in a distressed image. According to the observations of Figures 5 and 6, the optimal k is 2 and 3, while the optimal Δ_{rel} is 0.25 and 0.35 on detection and recognition tasks respectively.

4.6 Visualization Analysis

In this section, we attempt to understand the proposed approach through visualizations. All example images are from the CQU-BPDD test set.

4.6.1 CAM Visualization. We leverage Grad-CAM [26] to plot the Class Activation Maps (CAM) [44] of the image features extracted by the PicT and backbone Swin-S in Figure 4. We see that Swin-S does not achieve the desired results on pavement images. On the one hand, Swin-S loses some discriminative information at the patch level, since patch-level supervised information has still not been sufficiently mined, such as the CAMs in the third and fifth columns. On the other hand, its broad head makes the model more susceptible to interference by the complex pavement environment (see the first column) or causes dilution of the discriminative regions (see the fourth column). In contrast, PicT demonstrates the fuller patch-level information utilization and stronger discriminative power over Swin-S with our proposed modules.

4.6.2 Token Visualization. In Figure 7, we visualize the classification results of the tokens produced by *Patch Labeling Teacher* to investigate whether the token can characterize a 16×16 pixel patch of pavement image. We can observe that these tokens exhibit strong

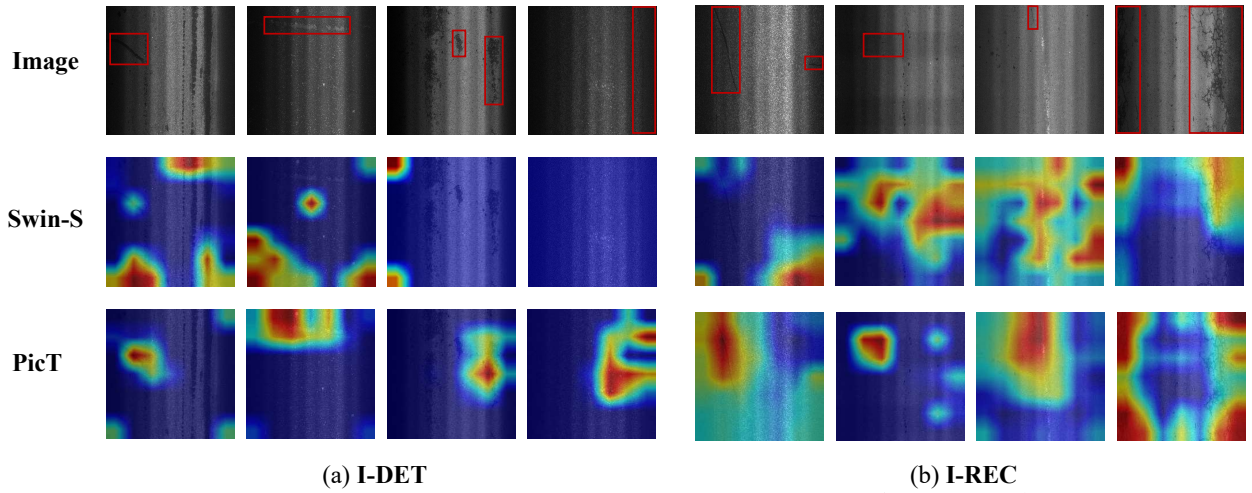


Figure 4: The CAM [44] visualization of feature maps produced by PicT and Swin-S (The baseline). The first row is the raw images, and the red rectangle marks the distressed area. Best viewed in color.

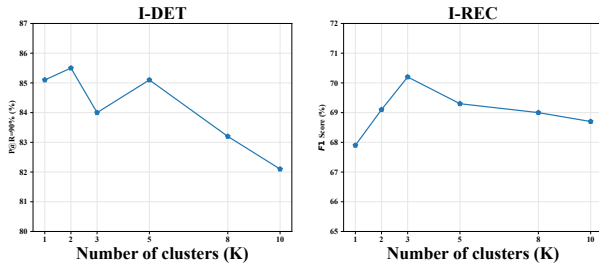


Figure 5: The performances of PicT under different k .

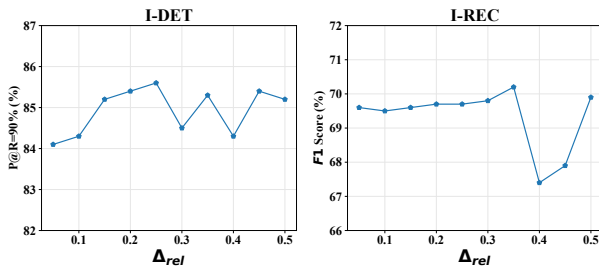


Figure 6: The performances of PicT under different Δ_{rel} .

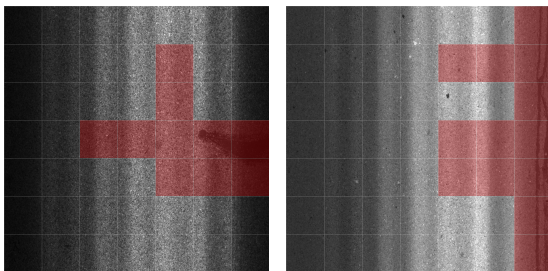


Figure 7: The visualization of tokens based on the patch classification results produced by *Patch Labeling Teacher*. The red mask indicates the distressed area predicted by the model. local discriminability despite the absence of any strong supervised information. We attribute this to the local representational ability of the visual tokens themselves, and the effectiveness of the weakly

supervised training module *Patch Labeling Teacher*. Token visualization results demonstrate that the weakly supervised *Patch Labeling Teacher* does indeed label the patches as designed. Moreover, it also explains how PicT profits from the patch-level classification branch to further improve the final classification performance.

5 CONCLUSION

In this work, we propose a slim weakly supervised vision Transformer (PicT) for pavement distress classification, achieving solid results on detection and recognition tasks. We show that PicT elegantly solves the efficiency and modeling problems of previous approaches. We also present that PicT is more suitable for pavement distress classification tasks than the general vision Transformer due to its adequate and rational utilization of patches information with quantitative and visualization analysis.

ACKNOWLEDGMENTS

This work was supported in part by the National Natural Science Foundation of China under Grant 62176030, and the Natural Science Foundation of Chongqing under Grant cstc2021jcyj-msxmX0568.

REFERENCES

- [1] Hangbo Bao, Li Dong, and Furu Wei. 2021. Beit: Bert pre-training of image transformers. *arXiv preprint arXiv:2106.08254* (2021).
- [2] Zhiyang Chen, Yousong Zhu, Chaoyang Zhao, Guosheng Hu, Wei Zeng, Jinqiao Wang, and Ming Tang. 2021. Dpt: Deformable patch-based transformer for visual recognition. In *Proceedings of the 29th ACM International Conference on Multimedia*. 2899–2907.
- [3] JaChing Chou, Wende A O’Neill, and HD Cheng. 1994. Pavement distress classification using neural networks. In *Proceedings of IEEE International Conference on Systems, Man and Cybernetics*, Vol. 1. IEEE, 397–401.
- [4] Jacob Devlin, Ming-Wei Chang, Kenton Lee, and Kristina Toutanova. 2018. Bert: Pre-training of deep bidirectional transformers for language understanding. *arXiv preprint arXiv:1810.04805* (2018).
- [5] Thomas G Dietterich, Richard H Lathrop, and Tomás Lozano-Pérez. 1997. Solving the multiple instance problem with axis-parallel rectangles. *Artificial intelligence* 89, 1-2 (1997), 31–71.
- [6] Hongwen Dong, Kechen Song, Yanyan Wang, Yunhui Yan, and Peng Jiang. 2021. Automatic Inspection and Evaluation System for Pavement Distress. *IEEE Transactions on Intelligent Transportation Systems* (2021).
- [7] Alexey Dosovitskiy, Lucas Beyer, Alexander Kolesnikov, Dirk Weissenborn, Xi-aohua Zhai, Thomas Unterthiner, Mostafa Dehghani, Matthias Minderer, Georg

- Heigold, Sylvain Gelly, et al. 2020. An image is worth 16x16 words: Transformers for image recognition at scale. *arXiv preprint arXiv:2010.11929* (2020).
- [8] Zhun Fan, Yuming Wu, Jiewei Lu, and Wenji Li. 2018. Automatic pavement crack detection based on structured prediction with the convolutional neural network. *arXiv preprint arXiv:1802.02208* (2018).
- [9] Xinyang Feng, Dongjin Song, Yuncong Chen, Zhengzhang Chen, Jingchao Ni, and Haifeng Chen. 2021. Convolutional Transformer based Dual Discriminator Generative Adversarial Networks for Video Anomaly Detection. In *Proceedings of the 29th ACM International Conference on Multimedia*. 5546–5554.
- [10] Wei Gao, Fang Wan, Xingjia Pan, Zhiliang Peng, Qi Tian, Zhenjun Han, Bolei Zhou, and Qixiang Ye. 2021. TS-CAM: Token Semantic Coupled Attention Map for Weakly Supervised Object Localization. In *Proceedings of the IEEE/CVF International Conference on Computer Vision*. 2886–2895.
- [11] Rohit Girdhar, Joao Carreira, Carl Doersch, and Andrew Zisserman. 2019. Video action transformer network. In *Proceedings of the IEEE/CVF Conference on Computer Vision and Pattern Recognition*. 244–253.
- [12] Kasthurirangan Gopalakrishnan, Siddhartha K Khaitan, Alok Choudhary, and Ankit Agrawal. 2017. Deep convolutional neural networks with transfer learning for computer vision-based data-driven pavement distress detection. *Construction and Building Materials* 157 (2017), 322–330.
- [13] John A Hartigan and Manchek A Wong. 1979. Algorithm AS 136: A k-means clustering algorithm. *Journal of the royal statistical society. series c (applied statistics)* 28, 1 (1979), 100–108.
- [14] Dailan He, Yusheng Zhao, Junyu Luo, Tianrui Hui, Shaofei Huang, Aixi Zhang, and Si Liu. 2021. TransRefer3D: Entity-and-Relation Aware Transformer for Fine-Grained 3D Visual Grounding. In *Proceedings of the 29th ACM International Conference on Multimedia*. 2344–2352.
- [15] Ju He, Jie-Neng Chen, Shuai Liu, Adam Kortylewski, Cheng Yang, Yutong Bai, Changhu Wang, and Alan Yuille. 2021. Transfg: A transformer architecture for fine-grained recognition. *arXiv preprint arXiv:2103.07976* (2021).
- [16] Kaiming He, Xinlei Chen, Saining Xie, Yanghao Li, Piotr Dollár, and Ross Girshick. 2021. Masked autoencoders are scalable vision learners. *arXiv preprint arXiv:2111.06377* (2021).
- [17] Kaiming He, Xiangyu Zhang, Shaoqing Ren, and Jian Sun. 2016. Deep residual learning for image recognition. In *Proceedings of the IEEE conference on computer vision and pattern recognition*. 770–778.
- [18] Yunqing Hu, Xuan Jin, Yin Zhang, Haiwen Hong, Jingfeng Zhang, Yuan He, and Hui Xue. 2021. RAMS-Trans: Recurrent Attention Multi-scale Transformer for Fine-grained Image Recognition. In *Proceedings of the 29th ACM International Conference on Multimedia*. 4239–4248.
- [19] Guixin Huang, Sheng Huang, Luwen Huangfu, and Dan Yang. 2021. Weakly Supervised Patch Label Inference Network with Image Pyramid for Pavement Diseases Recognition in the Wild. In *ICASSP 2021-2021 IEEE International Conference on Acoustics, Speech and Signal Processing (ICASSP)*. IEEE, 7978–7982.
- [20] Sheng Huang, Wenhao Tang, Guixin Huang, Luwen Huangfu, and Dan Yang. 2022. Weakly Supervised Patch Label Inference Networks for Efficient Pavement Distress Detection and Recognition in the Wild. *arXiv preprint arXiv:2203.16782* (2022).
- [21] Lu Jiang, Zhengyuan Zhou, Thomas Leung, Li-Jia Li, and Li Fei-Fei. 2018. Mentor-net: Learning data-driven curriculum for very deep neural networks on corrupted labels. In *International Conference on Machine Learning*. PMLR, 2304–2313.
- [22] Baoxian Li, Kelvin CP Wang, Allen Zhang, Enhui Yang, and Guolong Wang. 2020. Automatic classification of pavement crack using deep convolutional neural network. *International Journal of Pavement Engineering* 21, 4 (2020), 457–463.
- [23] Jiangtong Li, Wentao Wang, Junjie Chen, Li Niu, Jianlou Si, Chen Qian, and Liqing Zhang. 2021. Video Semantic Segmentation via Sparse Temporal Transformer. In *Proceedings of the 29th ACM International Conference on Multimedia*. 59–68.
- [24] Ze Liu, Yutong Lin, Yue Cao, Han Hu, Yixuan Wei, Zheng Zhang, Stephen Lin, and Baining Guo. 2021. Swin transformer: Hierarchical vision transformer using shifted windows. *arXiv preprint arXiv:2103.14030* (2021).
- [25] Fereidoon Moghadas Nejad and Hamzeh Zakeri. 2011. An expert system based on wavelet transform and radon neural network for pavement distress classification. *Expert Systems with Applications* 38, 6 (2011), 7088–7101.
- [26] Ramprasaath R Selvaraju, Michael Cogswell, Abhishek Das, Ramakrishna Vedantam, Devi Parikh, and Dhruv Batra. 2017. Grad-cam: Visual explanations from deep networks via gradient-based localization. In *Proceedings of the IEEE international conference on computer vision*. 618–626.
- [27] Zhuchen Shao, Hao Bian, Yang Chen, Yifeng Wang, Jian Zhang, Xiangyang Ji, et al. 2021. Transmil: Transformer based correlated multiple instance learning for whole slide image classification. *Advances in Neural Information Processing Systems* 34 (2021).
- [28] Oriane Siméoni, Gilles Puy, Huy V Vo, Simon Roburin, Spyros Gidaris, Andrei Bursuc, Patrick Pérez, Renaud Marlet, and Jean Ponce. 2021. Localizing Objects with Self-Supervised Transformers and no Labels. *arXiv preprint arXiv:2109.14279* (2021).
- [29] Karen Simonyan and Andrew Zisserman. 2014. Very deep convolutional networks for large-scale image recognition. *arXiv preprint arXiv:1409.1556* (2014).
- [30] Kihyuk Sohn, David Berthelot, Nicholas Carlini, Zizhao Zhang, Han Zhang, Colin A Raffel, Ekin Dogus Cubuk, Alexey Kurakin, and Chun-Liang Li. 2020. Fixmatch: Simplifying semi-supervised learning with consistency and confidence. *Advances in Neural Information Processing Systems* 33 (2020), 596–608.
- [31] Christian Szegedy, Vincent Vanhoucke, Sergey Ioffe, Jon Shlens, and Zbigniew Wojna. 2016. Rethinking the inception architecture for computer vision. In *Proceedings of the IEEE conference on computer vision and pattern recognition*. 2818–2826.
- [32] Mingxing Tan and Quoc V Le. 2019. Efficientnet: Rethinking model scaling for convolutional neural networks. *arXiv preprint arXiv:1905.11946* (2019).
- [33] Wenhao Tang, Sheng Huang, Qiming Zhao, Ren Li, and Luwen Huangfu. 2021. An Iteratively Optimized Patch Label Inference Network for Automatic Pavement Distress Detection. *IEEE Transactions on Intelligent Transportation Systems* (2021).
- [34] Hugo Touvron, Matthieu Cord, Matthijs Douze, Francisco Massa, Alexandre Sablayrolles, and Hervé Jégou. 2021. Training data-efficient image transformers & distillation through attention. In *International Conference on Machine Learning*. PMLR, 10347–10357.
- [35] Ashish Vaswani, Noam Shazeer, Niki Parmar, Jakob Uszkoreit, Llion Jones, Aidan N Gomez, Łukasz Kaiser, and Illia Polosukhin. 2017. Attention is all you need. In *Advances in neural information processing systems*. 5998–6008.
- [36] Chaofan Wang, Aimin Sha, and Zhaoyun Sun. 2010. Pavement crack classification based on chain code. In *2010 Seventh international conference on fuzzy systems and knowledge discovery*, Vol. 2. IEEE, 593–597.
- [37] Enze Xie, Wenhao Wang, Zhiding Yu, Anima Anandkumar, Jose M Alvarez, and Ping Luo. 2021. SegFormer: Simple and efficient design for semantic segmentation with transformers. *Advances in Neural Information Processing Systems* 34 (2021).
- [38] Zhenda Xie, Zheng Zhang, Yue Cao, Yutong Lin, Jianmin Bao, Zhuliang Yao, Qi Dai, and Han Hu. 2021. Simmim: A simple framework for masked image modeling. *arXiv preprint arXiv:2111.09886* (2021).
- [39] Mengde Xu, Zheng Zhang, Han Hu, Jianfeng Wang, Lijuan Wang, Fangyun Wei, Xiang Bai, and Zicheng Liu. 2021. End-to-end semi-supervised object detection with soft teacher. In *Proceedings of the IEEE/CVF International Conference on Computer Vision*. 3060–3069.
- [40] Guowen Zhang, Pingping Zhang, Jinqing Qi, and Huchuan Lu. 2021. Hat: Hierarchical aggregation transformers for person re-identification. In *Proceedings of the 29th ACM International Conference on Multimedia*. 516–525.
- [41] Hao Zhang, Yanbin Hao, and Chong-Wah Ngo. 2021. Token shift transformer for video classification. In *Proceedings of the 29th ACM International Conference on Multimedia*. 917–925.
- [42] Yibo Zhang and J.P. Mohsen. 2018. A Project-Based Sustainability Rating Tool for Pavement Maintenance. *Engineering* 4, 2 (2018), 200–208. <https://doi.org/10.1016/j.eng.2018.03.001> Sustainable Infrastructure.
- [43] Zengqun Zhao and Qingshan Liu. 2021. Former-DFER: Dynamic Facial Expression Recognition Transformer. In *Proceedings of the 29th ACM International Conference on Multimedia*. 1553–1561.
- [44] Bolei Zhou, Aditya Khosla, Agata Lapedriza, Aude Oliva, and Antonio Torralba. 2016. Learning deep features for discriminative localization. In *Proceedings of the IEEE conference on computer vision and pattern recognition*. 2921–2929.
- [45] Jian Zhou, Peisen Huang, and Fu-Pen Chiang. 2005. Wavelet-based pavement distress classification. *Transportation research record* 1940, 1 (2005), 89–98.